Calhoun: The NPS Institutional Archive
DSpace Repository

Theses and Dissertations 1. Thesis and Dissertation Collection, all items

1998-06

Observed directional spectra of shoaling and breaking waves

Borbash, Matthew I.

Monterey, California. Naval Postgraduate School

http://hdl.handle.net/10945/8760

Downloaded from NPS Archive: Calhoun

Calhoun is the Naval Postgraduate School's public access digital repository for research materials and institutional publications created by the NPS community. Calhoun is named for Professor of Mathematics Guy K. Calhoun, NPS's first appointed -- and published -- scholarly author.

Dudley Knox Library / Naval Postgraduate School
411 Dyer Road / 1 University Circle
Monterey, California USA 93943

http://www.nps.edu/library

NPS ARCHIVE
1998.06
BORBASH, M.

DUDLEY KNOX LIBRARY
NAVAL POSTGRADUATE SCHOOL
MONTEREY, CA 93943-5101

DUDLEY KNOX LIBRARY
NAVAL POSTGRADUATE SCHOOL
MONTEREY CA 93943-5101

NAVAL POSTGRADUATE SCHOOL
Monterey, California

THESIS

OBSERVED DIRECTIONAL SPECTRA OF SHOALING AND BREAKING WAVES

by

Matthew I. Borbash

June, 1998

Thesis Advisor: T.H.C. Herbers

Approved for public release; distribution is unlimited.

REPORT DOCUMENTATION PAGE

Form Approved OMB No. 0704-0188

Public reporting burden for this collection of information is estimated to average 1 hour per response, including the time for reviewing instruction, searching existing data sources, gathering and maintaining the data needed, and completing and reviewing the collection of information. Send comments regarding this burden estimate or any other aspect of this collection of information, including suggestions for reducing this burden, to Washington Headquarters Services, Directorate for Information Operations and Reports, 1215 Jefferson Davis Highway, Suite 1204, Arlington, VA 22202-4302, and to the Office of Management and Budget, Paperwork Reduction Project (0704-0188) Washington DC 20503.

1. AGENCY USE ONLY *(Leave blank)*	2. REPORT DATE June, 1998	3. REPORT TYPE AND DATES COVERED Master's Thesis

4. TITLE AND SUBTITLE Observed Directional Spectra of Shoaling and Breaking Waves	5.FUNDING NUMBERS
6. AUTHOR(S) Matthew I. Borbash	
7. PERFORMING ORGANIZATION NAME(S) AND ADDRESS(ES) Naval Postgraduate School Monterey CA 93943-5000	8.PERFORMING ORGANIZATION REPORT NUMBER
9. SPONSORING/MONITORING AGENCY NAME(S) AND ADDRESS(ES)	10.SPONSORING/MONITORING AGENCY REPORT NUMBER

11. SUPPLEMENTARY NOTES The views expressed in this thesis are those of the author and do not reflect the official policy or position of the Department of Defense or the U.S. Government.

12a. DISTRIBUTION/AVAILABILITY STATEMENT Approved for public release; distribution is unlimited.	12b. DISTRIBUTION CODE

13. ABSTRACT *(maximum 200 words)*

The evolution of the frequency-directional wave spectrum, $E(f,\theta)$, across the inner continental shelf and beach was examined with measurements collected at the U.S. Army Corps of Engineer's Field Research Facility during the recent SandyDuck experiment. Arrays of bottom pressure sensors were deployed on the shelf in 20 m depth and on the beach in depths ranging from 2 - 5 m. These arrays were complemented by a directional wave buoy in 20 m depth and an array of pressure sensors in 8 m depth maintained by the U.S. Army Corps of Engineers. A preliminary analysis of these data is presented here focused on four case studies that illustrate the observed wave shoaling evolution in both non-breaking and breaking conditions. Estimates of $E(f,\theta)$ extracted from array cross-spectra at six cross-shore locations are compared to predictions of linear refraction theory. The present observations support conclusions from previous studies that the cross-shore evolution of dominant wave propagation direction is well described by linear refraction theory. Observations of harmonic peak development at directions aligned with the dominant waves are consistent with theoretical wave-wave interaction rules and previous observations. In both non-breaking and breaking conditions, the observed $E(f,\theta)$ are directionally broader than predicted. In contrast to previous observations on a barred beach, the present observations on a planar beach do not show a dramatic broadening of directional wave spectra in the surf zone.

14. SUBJECT TERMS Ocean Surface Gravity Waves, Directional Wave Spectra, Surf Zone, Wave Shoaling, Beach	15. NUMBER OF PAGES 46
	16. PRICE CODE

17. SECURITY CLASSIFICATION OF REPORT Unclassified	18. SECURITY CLASSIFICATION OF THIS PAGE Unclassified	19. SECURITY CLASSIFICATION OF ABSTRACT Unclassified	20. LIMITATION OF ABSTRACT UL

NSN 7540-01-280-5500

Standard Form 298 (Rev. 2-89)
Prescribed by ANSI Std. 239-18 298-102

DUDLEY KNOX LIBRARY
NAVAL POSTGRADUATE SCHOOL
MONTEREY, CA 93943-5101

Approved for public release; distribution is unlimited.

OBSERVED DIRECTIONAL SPECTRA OF SHOALING AND BREAKING WAVES

Matthew I. Borbash
Lieutenant, United States Navy
B.S., North Carolina State University, 1992

Submitted in partial fulfillment
of the requirements for the degree of

MASTER OF SCIENCE IN METEOROLOGY AND PHYSICAL OCEANOGRAPHY

from the

NAVAL POSTGRADUATE SCHOOL
June, 1998

ABSTRACT

The evolution of the frequency-directional wave spectrum, $E(f,\theta)$, across the inner continental shelf and beach was examined with measurements collected at the U.S. Army Corps of Engineer's Field Research Facility during the recent SandyDuck experiment. Arrays of bottom pressure sensors were deployed on the shelf in 20 m depth and on the beach in depths ranging from 2 - 5 m. These arrays were complemented by a directional wave buoy in 20 m depth and an array of pressure sensors in 8 m depth maintained by the U.S. Army Corps of Engineers. A preliminary analysis of these data is presented here focused on four case studies that illustrate the observed wave shoaling evolution in both non-breaking and breaking conditions. Estimates of $E(f,\theta)$ extracted from array cross-spectra at six cross-shore locations are compared to predictions of linear refraction theory. The present observations support conclusions from previous studies that the cross-shore evolution of dominant wave propagation direction is well described by linear refraction theory. Observations of harmonic peak development at directions aligned with the dominant waves are consistent with theoretical wave-wave interaction rules and previous observations. In both non-breaking and breaking conditions, the observed $E(f,\theta)$ are directionally broader than predicted. In contrast to previous observations on a barred beach, the present observations on a planar beach do not show a dramatic broadening of directional wave spectra in the surf zone.

TABLE OF CONTENTS

I. INTRODUCTION 1

II. FIELD EXPERIMENT AND DATA ANALYSIS 5

III. OBSERVATIONS 11

IV. SUMMARY 17

APPENDIX 19

LIST OF REFERENCES 33

INITIAL DISTRIBUTION LIST 35

ACKNOWLEDGEMENTS

This research was funded by the Office of Naval Research, Coastal Dynamics Program. The field experiment was conducted in collaboration with Dr. Steve Elgar (Washington State University) and Dr. R.T. Guza (Scripps Institution of Oceanography). The tireless efforts of the staff of the Scripps Institution of Oceanography Center for Coastal Studies during the deployment of 100+ instruments is greatly appreciated. Nearshore bathymetry and 8 m depth array data were provided by the Field Research Facility of the U.S. Army Engineer Waterways Experiment Station's Coastal Engineering Research Center. Permission to use these data is appreciated.

Sincere gratitude is extended to my advisor, Thomas Herbers, for his guidance and instruction during my pursuit of this effort. Paul Jessen provided exceptional technical assistance. My wife, Brittney, gave tremendous support and encouragement.

I. INTRODUCTION

Accurate predictions of the nearshore transformation of ocean waves are vital to naval littoral operations (e.g., mine warfare, amphibious landings, swimmer operations) and civilian coastal erosion studies. As waves propagate from the open ocean onto shallow coastal shelves and ultimately break on beaches, linear and nonlinear effects change their amplitudes and directional characteristics. The present study is focused on the still poorly understood transformation of the directional properties of waves propagating across the inner shelf and beach.

Linear shoaling of waves is well understood. Reduction of the group speed in shallow water generally causes an amplification of wave amplitudes on beaches. Waves arriving at an oblique angle relative to the shore are refracted toward normal incidence while for large incidence angles their amplitudes are reduced (e.g., Kinsman, 1965).

Close to shore, strong nonlinearities and wave breaking affect the frequency spectra and directional properties of waves. Nonlinear interaction between two primary wave components with frequencies f_1 and f_2 and vector wavenumber $\mathbf{k}_1$ and $\mathbf{k}_2$ excite a secondary wave component with the sum frequency (f_1+f_2) and wavenumber $(\mathbf{k}_1+\mathbf{k}_2)$. If the incident wave spectrum is narrow (i.e., $f_1 \approx f_2$, $\mathbf{k}_1 \approx \mathbf{k}_2$), these secondary waves are harmonic components with approximately twice the frequency of the incident waves and propagate in approximately the same direction as the incident waves (Freilich et al. 1990; Herbers et al. 1998). Subsequent interactions between the primary waves and the newly formed secondary waves excite higher harmonic components ($3f_1$, $4f_1$, ...) all approximately directionally aligned with the incident waves.

Field observations of the shoaling evolution of directional wave spectra are scarce. Freilich et al. (1990) presented high resolution directional spectrum estimates obtained from two arrays of pressure sensors located well outside the surf zone on a nearly planar, natural beach. These observations show the expected refraction toward normal incidence of incident swells and energy transfers to directionally aligned harmonics. In bimodal spectra, with two distinct wave systems arriving at the beach from different incidence angles, the theoretically expected excitation of waves at the sum frequency and vector wavenumber was observed. Herbers et al. (1998) presented estimates of mean directions and directional spreading parameters extracted from cross-shore transects of co-located pressure sensors and current meters on barred and non-barred beaches. These observations show that although the mean wave direction does not appear to be strongly influenced by wave breaking, the directional spreading of waves increases significantly in the surf zone on both barred and non-barred beaches.

In the present study, a preliminary analysis is presented of a more extensive shoaling wave data set acquired during the SandyDuck experiment near Duck, NC. Six high resolution arrays of bottom pressure sensors were deployed for four months along a transect extending from the inner shelf through the surf zone. These measurements provide unique detailed estimates of the shoaling and breaking transformation of directional wave spectra. The field experiment and data analysis techniques are described in chapter II. Four case studies spanning a range of conditions (i.e., nonbreaking and breaking waves, narrow swell spectra, and broad wind seas) are described in chapter III.

The results are summarized in chapter IV.

II. FIELD EXPERIMENT AND DATA ANALYSIS

Detailed measurements of the evolution of frequency-directional wave spectra across the inner continental shelf and beach were collected during the SandyDuck experiment at the U.S. Army Corps of Engineer's Field Research Facility located near Duck, NC, on a straight barrier island. This site is fully exposed to the Atlantic Ocean and features an 80 km wide, shallow (20 - 50 m depths) shelf. Arrays of pressure sensors were deployed on the inner shelf in 20 m depth (5 km from shore) and on the beach in depths ranging from 2 - 5 m (Figure 1). The experiment was conducted in collaboration with Dr. Steve Elgar (Washington State University) and Dr. R. T. Guza (Scripps Institution of Oceanography). High-quality wave data were collected at all instrument locations during a four month period (August - November 1997).

The 20 m depth array consisted of nine pressure sensors arranged in a 500 m equilateral triangle (Figure 2, bottom). The pressure sensors are battery powered, internal recording instruments mounted rigidly near the sea floor inside anchors. The autonomous instruments were synchronized to within 10 ms using accurate temperature compensated oscillators and thus can be used as a coherent array for sea and swell waves. The sample frequency was 2 Hz. Instruments were accurately positioned using differential GPS, an underwater acoustic navigation system, and direct underwater tape measurements. Sensor spacing uncertainties range from about 0.4 m for the shortest array legs to 2.0 m for the longest array legs. The array geometry allowed for omni-directional wave measurements. Sensor spacings ranging from 20 m to 300 m were chosen to accurately resolve swell and sea waves in the frequency range 0.04 Hz - 0.2 Hz. Waves with frequencies higher than 0.2 Hz are strongly attenuated at the sea floor, and thus not accurately measured by the pressure sensors (e.g., Herbers and Guza, 1991). A Datawell Directional Waverider buoy was deployed within the array perimeter to provide measurements of the high frequency part (0.2 Hz - 0.5 Hz) of the wave spectrum. This surface-following buoy measures 3-component accelerations that yield wave frequency spectra and low-resolution directional information (e.g., Long, 1980). Buoy data sampled with a frequency of 1.28 Hz was transmitted continuously via an HF radio link to a receiver on shore.

The nearshore instrumentation included four arrays of 10 or 11 bottom-mounted pressure sensors, each with an alongshore aperture of 210 m and a cross-shore aperture of 35 m (Figure 2, top). The arrays were positioned at offshore distances (relative to F.R.F. coordinates) of 210, 260, 375, and 500 m in nominal depths of 2.9, 3.7, 3.9, and 5.1 m, respectively. The nearshore arrays also included sonar altimeters that provided accurate, continuous water depth measurements (Gallagher et al. 1996). All instruments were cabled to a central data acquisition center onshore. The sample rate of the pressure sensors was 2 Hz.

Additional directional wave data were available from a permanent array of pressure sensors (maintained by the U.S. Army Corps of Engineers Field Research Facility) located about 900 m from shore in 8 m depth (Figure 2, middle). The 15-element array with an aperture of 250 m (alongshore) x 120 m (cross-shore) and a 2 Hz sample rate resolves waves with frequencies up to approximately 0.3 Hz.

Bathymetry at the site is characterized by a gently sloping (≈1:250), nearly planar inner shelf (Figure 1) and a slightly steeper ($\approx$1:100) beach (Figure 3). Seaward of the 20 m array, the shelf is characterized by a very gentle slope ($\approx$1:2500) with large (scales O(5 km)) ridge-like features that have vertical scales of O(5 m). Refraction computations show that the effects of the benign shelf topography on wave transformation across the shelf are significant, but do not produce strong local gradients in wave energy (Hendrickson, 1996). Daily bathymetric surveys of the nearshore region (e.g., Figure 3) indicate that the beach changes over the course of the experiment were small. The sand bar located 300 m offshore (Figure 3) remained relatively stationary with its crest submerged about 5 m below mean sea level, and did not strongly affect the wave shoaling process. Close to shore, the morphology was more dynamic, with the development of transient bars and alongshore depth variations. These changes occurred well shoreward of the nearshore arrays, and thus did not influence this study.

In the following analysis of wave shoaling evolution from 20 to 2.5 m depth, alongshore depth variations are neglected. The preliminary analysis presented here is focused on four 3-hour-long case studies that illustrate the observed wave shoaling evolution in both non-breaking and breaking conditions. Prior to the analysis, the data were tested for stationarity and spatial homogeneity using a variety of methods. Temporal changes in 2-minute average wave variances were used to ensure stationarity of wave conditions throughout the selected 3-hour-long record. Alongshore homogeneity over the alongshore extent of the nearshore arrays was verified by intercomparing the measured spectra of each sensor in the array, as well as the coherence and phase spectra of redundant alongshore sensor pairs. For example, the southernmost sensors of the nearshore arrays consistently recorded spectral density values an order of magnitude lower than other array sensors for waves arriving from large, oblique southerly directions. These discrepancies are likely caused by the close proximity of the U.S. Army Corps of Engineer's research pier (e.g., wave blocking by pier pilings), and therefore data from the southernmost sensors was not used.

Array cross-spectra were calculated based on Fourier transforms of overlapping 1024 s segments. Merging 11 frequency bands resulted in estimates with a frequency resolution of 0.0107 Hz and 220 degrees of freedom. For each frequency, f, the corresponding directional distribution of wave energy, $S(\theta;f)$, was estimated from the array cross-spectra using the variational technique described in Herbers and Guza (1990). The direction θ is defined relative to the local shoreline orientation with $\theta = 0^\circ$ corresponding to normal incidence to the beach (waves arriving from 70° true N), and θ is positive (negative) for waves approaching the beach from northerly (southerly) directions. The method yields the smoothest non-negative distribution function that is statistically consistent with the observations. This roughness minimization technique effectively suppresses spurious peaks in $S(\theta;f)$ estimates that might otherwise be misinterpreted as multimodal features of the directional wave spectrum. The estimates of $S(\theta;f)$ were combined with an estimate of the surface elevation frequency spectrum $E(f)$ (obtained by averaging the measured auto-spectra and applying a linear theory depth correction) to form the wave frequency-directional spectrum $E(f,\theta)$ ($= E(f)S(\theta;f)$).

Estimates of $E(f,\theta)$ were initially computed at all array locations using the full array geometry (i.e., both the alongshore and cross-shore legs). Spurious peaks and poor convergence of $S(\theta;f)$ estimates at high frequencies observed at the nearshore and 8 m depth locations, suggest that nonlinear and/or wave breaking effects contributed significant errors. The estimation technique assumes a linear dispersion relation, and thus is sensitive to nonlinear changes in the wavenumber (e.g., amplitude dispersion and bound waves). Wave-breaking induced energy losses may reduce the coherence in the cross-shore array legs causing additional inversion problems. Frequency-directional spectra at the nearshore and 8 m depth locations were subsequently re-computed using only the alongshore legs of the arrays. These linear array estimates are insensitive to dispersion errors and cross-shore inhomogeneities, but cannot distinguish shoreward propagating waves ($-90^\circ<\theta<90^\circ$) from seaward propagating waves ($90^\circ<\theta<270^\circ$). Since the full array estimates already confirmed that swell reflections from shore were weak, the $S(\theta;f)$ estimates obtained from the linear arrays were constrained to vanish at seaward propagation directions ($90^\circ<\theta<270^\circ$) (Herbers and Guza, 1990). The resulting estimates were nearly identical to the full array estimates in the energetic part of the spectrum and smooth at higher frequencies. In two cases, August 17 and October 19, estimates of $E(f,\theta)$ extracted from the 20 m depth array measurements also indicated spurious structure and convergence problems at high frequencies. The estimates were recomputed using a five element, linear sub-array. In the August 17 case, with waves arriving from southerly angles, the northern leg of the triangle array was used with the constraint $S(\theta;f) = 0$ at angles ($-180^\circ<\theta<-150^\circ$, $30^\circ<\theta<180^\circ$). Similarly, for the October 19 case with waves arriving from northerly directions, the southern leg of the triangle array was used with the constraint $S(\theta;f) = 0$ at angles ($-180^\circ<\theta<-30^\circ$, $150^\circ<\theta<180^\circ$).

Estimates of $E(f,\theta)$ in 20 m depth over a wider frequency range (0.04 - 0.5 Hz) were obtained from the directional wave buoy using the Maximum Entropy Method described by Lygre and Krogstad (1986). This method yields a unimodal or bimodal $S(\theta;f)$ that exactly fits the measured buoy cross-spectra. Directional resolution is limited because the buoy cross-spectra define only four moments of $S(\theta;f)$. The buoy spectral analysis is based on an ensemble average of 54 data segment with lengths of 200 s. The resulting $E(f,\theta)$ estimates with 0.005 Hz frequency resolution were smoothed to the same resolution as the array estimates. At low frequencies where they overlap, the array and buoy estimates are in good agreement. The final estimates of $E(f,\theta)$ in 20 m depth were formed by matching the array estimates in the frequency range 0.04 - 0.2 Hz with the buoy estimates in the frequency range 0.2 - 0.5 Hz.

III. OBSERVATIONS

Example observations of the shoaling evolution of E(f,θ) are shown in Figures 4 - 11. The four cases described in detail below span a wide range of conditions, including normal and large oblique incidence angles and both non-breaking and breaking conditions. In order to distinguish linear refraction effects from nonlinear harmonic generation and surf zone effects, the observed evolution of E(f,θ) was compared to simple linear theory predictions. On a beach with straight and parallel depth contours, the transformation of E(f,θ) is governed by

$$E_s(f,\theta_s) = \frac{C_d C_{gd}}{C_s C_{gs}} E_d(f,\theta_d) \qquad (1)$$

(Longuet-Higgins, 1957; LeMéhauté and Wang, 1982), where subscripts d and s denote wave properties at a deeper and shallower cross-shore location, C and C_g represent the wave phase and group speed, and the angles θ_d and θ_s are given by Snell's Law

$$\sin(\theta_s) = \frac{C_s}{C_d} \sin(\theta_d) \qquad (2)$$

Eqs (1) and (2) were used to transform the 20 m depth estimates of E(f,θ) to each of the shallower array locations. The resulting predictions are included in Figures 4 - 11.

A. AUGUST 17

The August 17 conditions are characterized by a steady oblique-offshore wind with a speed of 8 m/s and direction of -140°. Significant wave heights were less than 0.5 m at all array locations and breaking occurred in the region shoreward of the shallowest array. Frequency-directional wave spectra observed at the six arrays are compared to the linear refraction predictions in Figure 4. Observed and predicted directional distributions of energy at selected frequencies are compared in Figure 5. In 20 m depth, the wave spectrum in the dominant 0.15 - 0.30 Hz range is broad in frequency and directionally narrow with waves propagating at large southerly incidence angles nearly parallel to the shore. These waves are strongly refracted over the inner shelf and beach, and the observed changes in wave direction are well described by the linear refraction predictions. High frequency spectral energy levels are reduced by about a factor 5 between the deepest and shallowest sites, consistent with predicted spectral levels (left panels). The observed refraction of the smaller and broader 0.1 Hz swell peak from -50° at the deepest site to -20° at the shallowest site is also in agreement with the prediction (Figure 5, left panels). This peak is amplified during shoaling and dominates the wave spectrum at the shallower sites (Figure 4), in agreement with the prediction. Whereas observed energy levels and mean propagation directions are in good agreement with the predictions, the observed $S(\theta;f)$ are broader than the predicted extremely narrow $S(\theta;f)$ (e.g., 0.17 Hz in Figure 5). Possible explanations for these discrepancies are the limited directional resolution of the array and alongshore variations in wave directions caused by small alongshore depth variations that might broaden the array estimates of $S(\theta;f)$.

B. OCTOBER 2

The shoaling evolution of a more energetic wave field was observed on October 2 and is detailed in Figures 6 and 7. Conditions are characterized by a steady onshore wind with a speed of 11 m/s and a direction of 55°. In 20 m depth, $E(f,\theta)$ is relatively narrow in both frequency and direction with a single peak at approximately $f = 0.17$ Hz that is closely aligned with the wind direction (bottom panels of Figures 6 and 7). At higher frequencies, the $S(\theta;f)$ estimates (extracted from the directional wave buoy) are bimodal and approximately symmetric about the wind direction. The separation of the two peaks increases with frequency, similar to recent observations by Young et al. (1995) and Ewans (1998). Young et al. (1995) show that the bimodal structure of $E(f,\theta)$ at high frequencies can be explained with theoretical predictions of transfers of energy to higher frequencies through nonlinear wave-wave interactions. However, the 8 m depth array estimate of $E(f,\theta)$ shows high frequency waves propagating in the local wind direction and suggest that the bimodal distributions estimated from the buoy data may be erroneous. Errors in the directional buoy estimates of $S(\theta;f)$ at high frequencies may be introduced through nonlinearities in the buoy response or the inherent lack of resolution of directional buoys that measure only four integral moments of $S(\theta;f)$ (e.g., Herbers and Guza, 1990).

The observed significant wave height at the shallowest array is about 10% smaller than the predicted value, indicating that the surf zone is confined to a region shoreward of the shallowest array (upper left panel in Figure 6). The dominant sea peak is strongly refracted over the inner shelf and beach, and the observed changes in wave direction are well described by the linear refraction predictions. Similar to the previous case, the predicted refracted peaks are directionally narrower than the observed peaks (left panels in Figure 7). At two times the spectral peak frequency (0.34 Hz) the $E(f,\theta)$ observed at the shallower arrays are bimodal with one peak ($\theta \approx 50^\circ$) aligned with the wind direction and the expected harmonic peak ($\theta \approx 20^\circ$) aligned with the primary 0.17 Hz sea peak (Figure 6). This harmonic peak is strongly amplified during shoaling and dominates the high-frequency spectrum in 2.9 m depth (Figure 6).

C. NOVEMBER 1

The November 1 case (Figures 8 and 9) is characterized by a steady oblique offshore wind with a speed of 7 m/s and direction of -140°, similar to the August 17 case. Observed significant wave heights ranging from 1.2 m at the deepest array to 1.1 m at the shallowest array are close to the linear theory predictions (left panels in Figure 8) indicating that breaking occurred in the region shoreward of the shallowest location. In 20 m depth, the $E(f,\theta)$ estimate features a dominant 0.10 Hz peak with a large southerly incidence angle (-60°). The high frequency part of the spectrum is directionally narrower, with even larger, almost shore-parallel southerly angles (-80°), similar to the August 17 case. The strong refraction over the inner shelf and beach of the dominant wave direction is again well described by the linear refraction predictions (Figure 9, left panels). As in the previous cases, predicted directional distributions are narrower than observed at the shallower arrays. At high frequencies, second (0.2 Hz) and third (0.3 Hz) harmonic peaks are observed at the shallower sites which are approximately directionally aligned with the dominant (0.1 Hz) waves (Figure 8). Similar to the October 2 case, these harmonic peaks are amplified between 5.5 and 2.8 m depths and dominate the directional distributions at high frequencies at the shallowest array (Figure 9, center and right panels).

D. OCTOBER 19

The most energetic waves in the SandyDuck experiment were observed on October 19 (Figures 10 and 11) during a severe Nor'easter with maximum sustained wind speeds of about 17 m/s. The surf zone extended several kilometers offshore with a significant wave height at the 20 m depth array of about 3.9 m, decreasing steadily to 1.56 m at the shallowest array. Propagation directions of the dominant 0.1 Hz waves are nearly normal to the beach in 20 m depth and virtually unchanged throughout the surf zone (Figure 11, left panels) even though spectral energy levels are reduced by more than an order of magnitude at the shallowest array (Figure 10, left panels). The directional distributions are slightly broader than predicted with linear refraction theory at the shallower arrays, but the broadening of $S(\theta;f)$ is much less pronounced than that observed by Herbers et al. (1998) for comparably energetic waves breaking on a shallow bar. At twice the spectral peak frequency (0.19 Hz), the observed spectra show a transition from wind seas in 20 m depth (propagating in the local wind direction $\theta \approx 80°$) to second harmonic waves that are aligned with the dominant wave direction ($\theta \approx 0°$). In 8.2 m depth the sea and harmonic peaks are approximately equal in magnitude, and at the shallowest arrays the sea waves are completely submerged in the harmonic energy levels. A similar transition from wind-generated seas to harmonic waves is observed at 0.29 Hz (Figure 11, right panels). As in the August 17 case, the bimodal $S(\theta;f)$ observed in 21.2 m depth may be a directional buoy artifact rather than a true feature of the wave field. In 8.2 m depth, a refracting sea peak from 40° co-exists with a developing third harmonic peak at 5° (aligned with the dominant waves). This harmonic peak broadens during shoaling and dominates the spectrum at the shallower arrays.

IV. SUMMARY

The evolution of the frequency-directional wave spectrum, $E(f,\theta)$, across the inner continental shelf and beach was examined with extensive measurements collected at the Army Corps of Engineer's Field Research Facility near Duck, NC during the recent SandyDuck experiment. The barrier island field site is characterized by a straight coastline with a gently sloping (1:250) sandy bottom and weak alongshore depth variations. Arrays of bottom pressure sensors were deployed on the inner shelf in 20 m depth (5 km from shore) and on the beach in depths ranging from 2 - 5 m (Figure 1). A directional wave buoy was added to the 20 m depth array to measure high frequency seas that are attenuated at the sea bed. The SandyDuck arrays were complemented by a permanent array of pressure sensors in 8 m depth maintained by the Army Corps of Engineers. High-quality wave data were collected nearly continuously at all instrument locations during a four month period (August - November 1997).

The preliminary analysis presented here is focused on four case studies that span a range of conditions and illustrate the observed wave shoaling evolution in both non-breaking and breaking conditions. Smooth estimates of $E(f,\theta)$ were estimated from the cross-spectra of six arrays using the variational technique described in Herbers and Guza (1990). In 20 m depth, the array estimates of $E(f,\theta)$ at low frequencies were combined with buoy estimates at high frequencies obtained with the Maximum Entropy Method described in Lygre and Krogstad (1986). In all four case studies, the cross-shore evolution of the dominant wave propagation direction agrees well with simple linear theory predictions for wave refraction on a beach with straight and parallel depth contours. In the more energetic cases, the observed $E(f,\theta)$ show the development of harmonic peaks at the shallower sites with directions that are approximately aligned with the dominant waves (Figures 6, 8, 10), qualitatively consistent with theoretical wave-wave interaction rules and earlier observational studies (Freilich et al. 1990; Herbers et al. 1998).

In both non-breaking and breaking conditions, the observed $E(f,\theta)$ are directionally broader than the linear theory predictions, in particular when the incident wave field is directionally narrow (e.g., August 17, Figures 4, 5). These discrepancies may reflect the limited resolution of the arrays and/or alongshore variations in wave propagation directions associated with weak alongshore depth variations. Whereas Herbers et al. (1998) observed a sudden, dramatic directional broadening of wave spectra when waves broke on a shallow submerged sandbar, the present observations on a nearly planar beach do not indicate a strong wave breaking effect on directional wave properties. In fact, in the most energetic case (October 19) when the surf zone extended across the entire instrumented transect, the directional width of $E(f,\theta)$ remains nearly constant upon shoaling. These differences are possibly related to differences in nonlinear shoaling evolution and wave breaking characteristics (e.g., strongly localized breaking on a sand bar versus gradual breaking on a planar beach). Further work is needed to clarify the role of the sea bed profile in the shoaling evolution of directional wave properties.

APPENDIX

Figure 1. Plan view of the experiment site with locations of the nearshore, 8 m, and 20 m arrays and associated bathymetry (depth contours are relative to mean sea level).

Figure 2. Detailed plan view of the nearshore, 8 m, and 20 m arrays. Pressure sensors locations are represented by solid dots and the directional wave buoy location is indicated with a circle.

Figure 3. Representative beach topography during SandyDuck (courtesy of the Army Corps of Engineer's Field Research Facility). The bathymetry is characterized by a small shore-parallel bar located 275 m offshore and nearly straight and parallel depth contours. Bathymetry changes over the course of the experiment were weak with the exception of the dynamic beach face region shoreward of the nearshore arrays.

Figure 4. Wave shoaling evolution from 19.8 m depth (bottom panels) to 2.5 m depth (top panels) of small amplitude waves arriving from large oblique southerly angles on August 17, 1997. Observed (blue) and predicted (red) frequency spectra and significant wave heights are shown in the left panels. The color contour panels show the observed and predicted frequency-directional spectra at each array (units cm^2/Hz°; $\theta = 0^\circ$ corresponds to normal incidence to the beach) with the water depths indicated in the upper right corner .

Figure 5. Observed (solid) and predicted (dotted) directional distribution of wave energy at selected frequencies on August 17, 1997. Predictions at frequencies higher than

0.2 Hz (only measured with the directional wave buoy in 20 m depth) are omitted.

Figure 6. Wave shoaling evolution from 20.3 m depth (bottom panels) to 2.9 m depth (top panels) of moderately energetic waves arriving from large oblique northerly angles on October 2, 1997 (same format as Figure 4). The frequency-directional values are multiplied by f^3 to enhance the directional properties of high frequency waves.

Figure 7. Observed (solid) and predicted (dotted) directional distribution of wave energy at selected frequencies on October 2, 1997 (same format as Figure 5). The local wind direction is indicated with a dashed vertical line.

Figure 8. Wave shoaling evolution from 20.8 m depth (bottom panels) to 2.8 m depth (top panels) of moderately energetic waves arriving from oblique southerly angles on November 1, 1997 (same format as Figure 4). The frequency-directional values are multiplied by f^3 to enhance the directional properties of high frequency waves.

Figure 9. Observed (solid) and predicted (dotted) directional distribution of wave energy at selected frequencies on November 1, 1997 (same format as Figure 5).

Figure 10. Wave shoaling evolution from 21.2 m depth (bottom panels) to 3.3 m depth (top panels) of large amplitude waves arriving from directions close to normal incidence on October 19, 1997 (same format as Figure 4).

Figure 11. Observed (solid) and predicted (dotted) directional distribution of wave energy at selected frequencies on October 19, 1997 (same format as Figure 5). The local wind direction is indicated with a dashed vertical line.

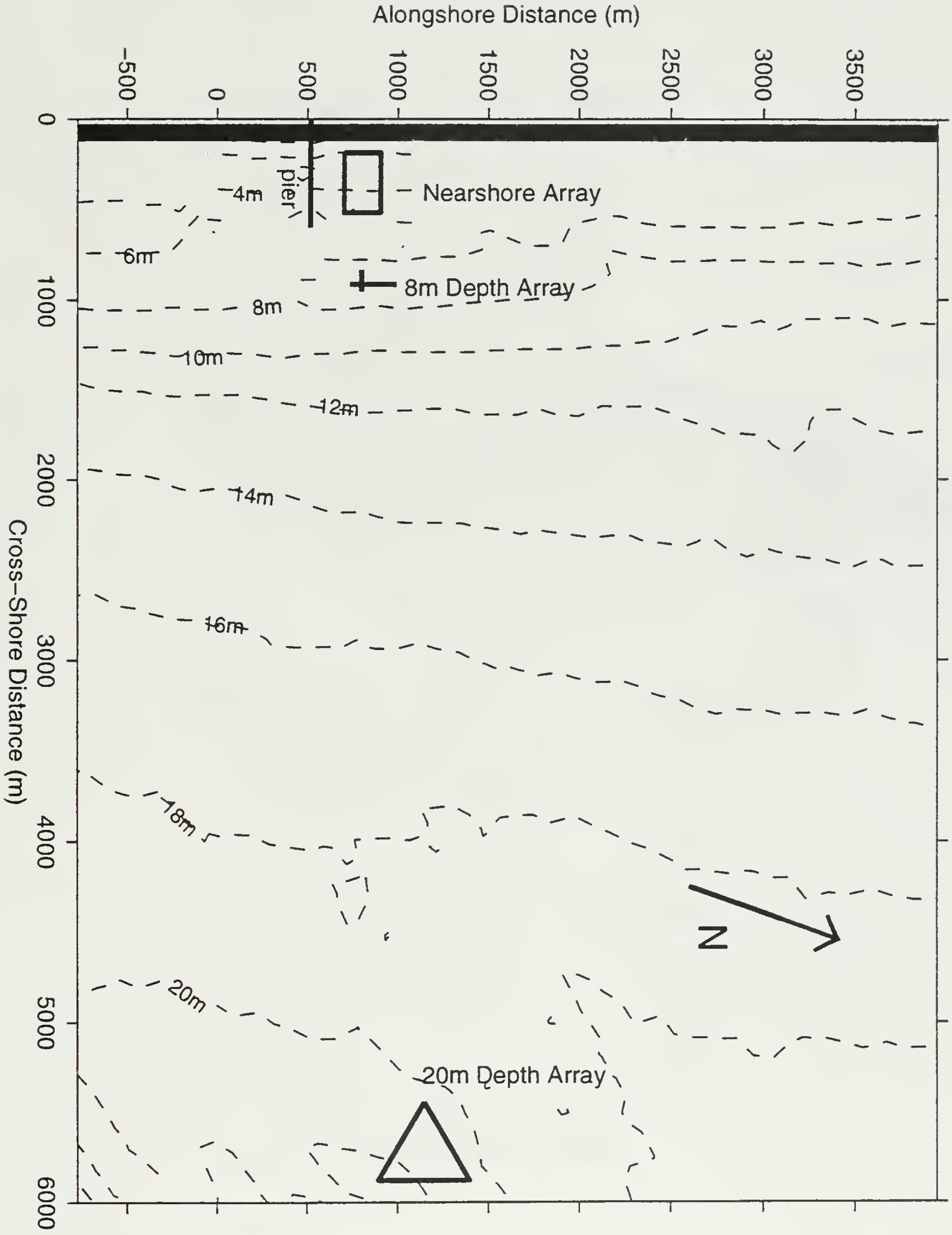
Alongshore Distance (m)
-500
0
500
1000
1500
2000
2500
3000
3500
Cross-Shore Distance (m)
0
1000
2000
3000
4000
5000
6000
pier
Nearshore Array
8m Depth Array
20m Depth Array
4m
6m
8m
10m
12m
14m
16m
18m
20m
N

Figure 1

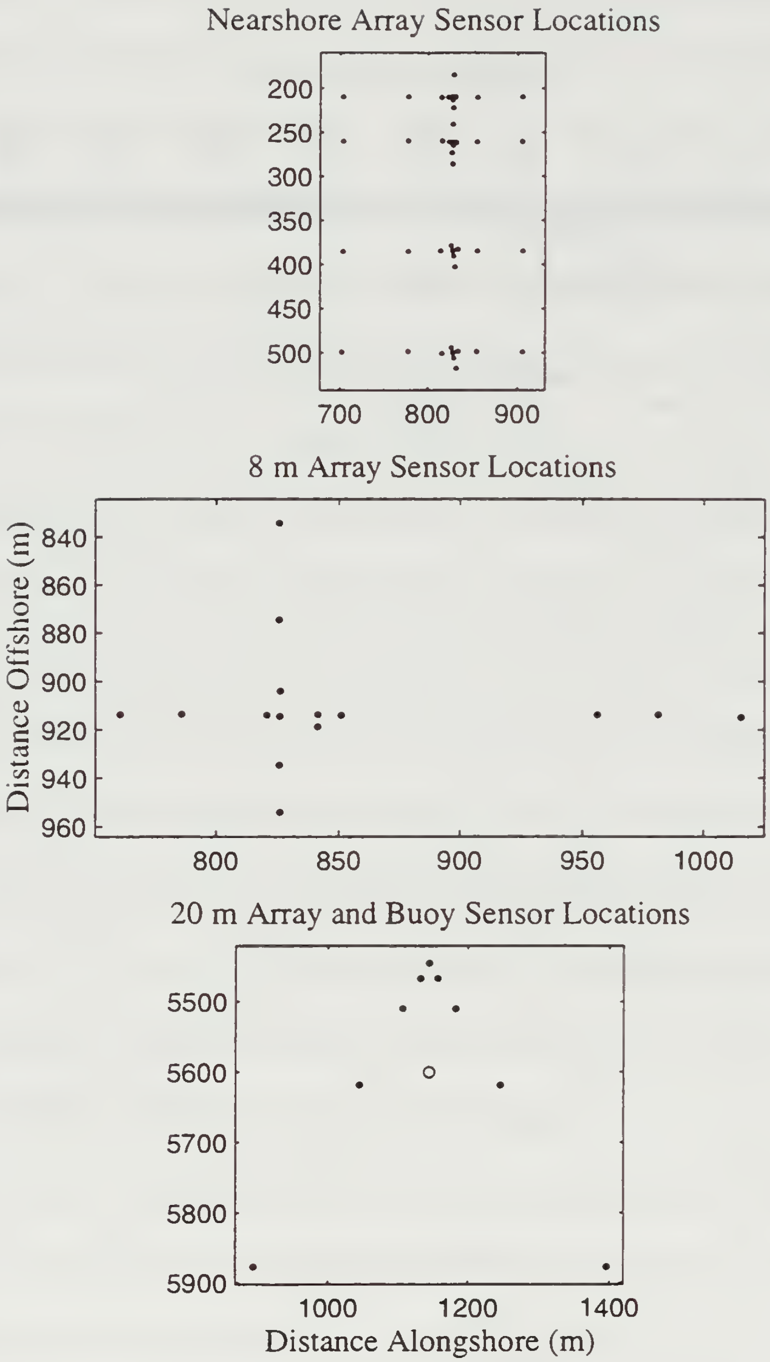
Nearshore Array Sensor Locations
200
250
300
350
400
450
500
700
800
900
8 m Array Sensor Locations
Distance Offshore (m)
840
860
880
900
920
940
960
800
850
900
950
1000
20 m Array and Buoy Sensor Locations
5500
5600
5700
5800
5900
1000
1200
1400
Distance Alongshore (m)

Figure 2

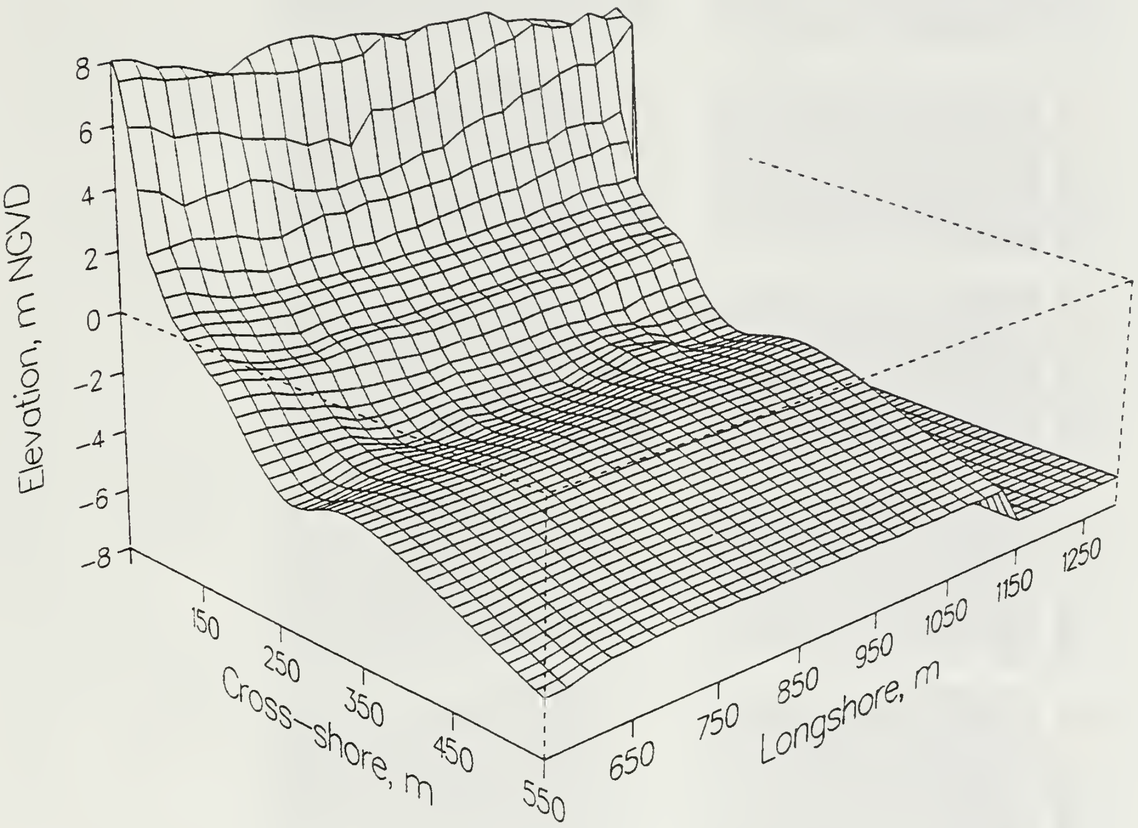
Elevation, m NGVD
8
6
4
2
0
-2
-4
-6
-8
Cross-shore, m
150
250
350
450
550
Longshore, m
650
750
850
950
1050
1150
1250

Figure 3

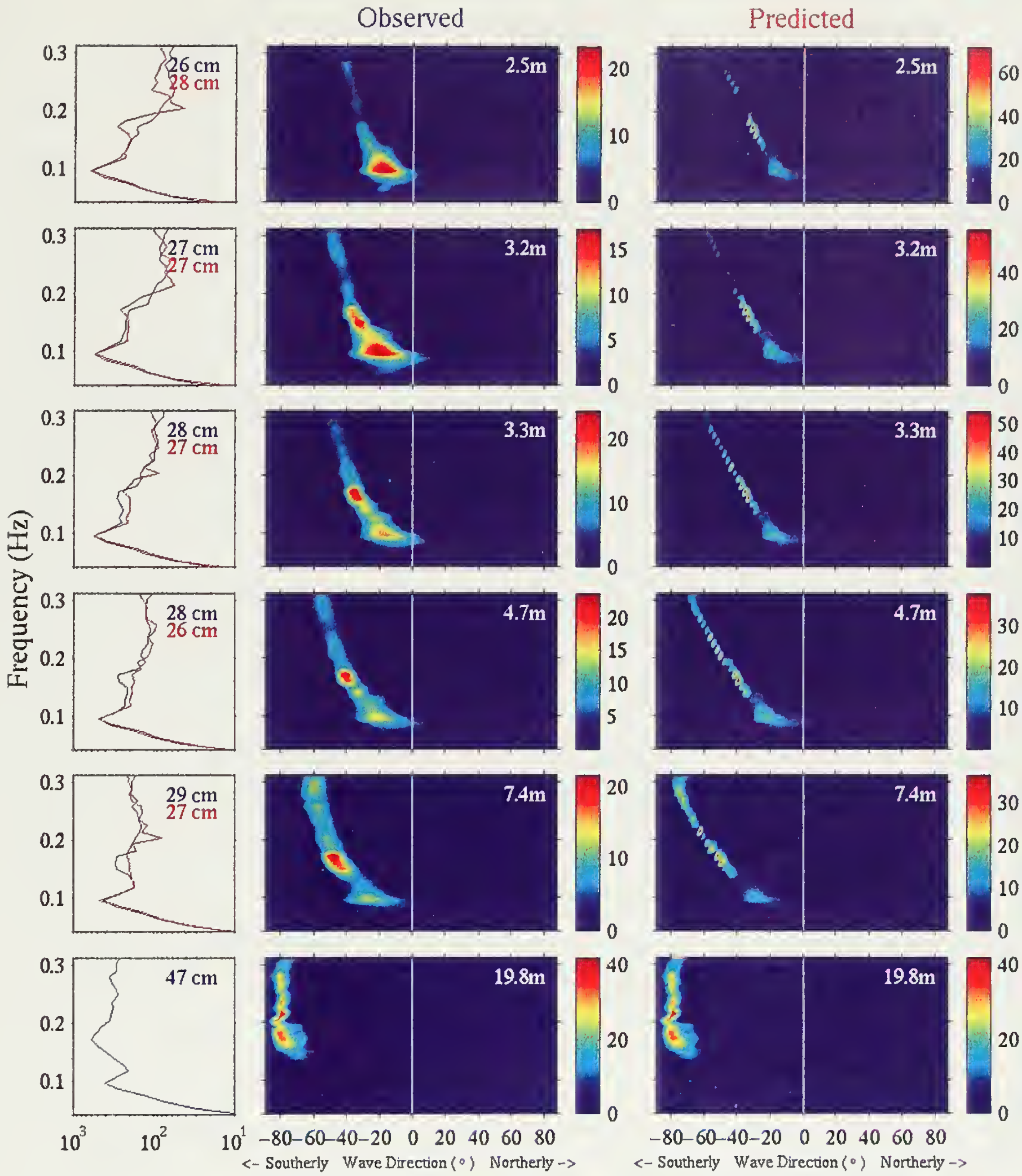
Observed
Predicted
Frequency (Hz)
0.3
0.2
0.1
26 cm
28 cm
27 cm
27 cm
28 cm
27 cm
28 cm
26 cm
29 cm
27 cm
47 cm
2.5m
3.2m
3.3m
4.7m
7.4m
19.8m
10³ 10² 10¹
−80 −60 −40 −20 0 20 40 60 80
<- Southerly Wave Direction (°) Northerly ->
0 10 20
0 5 10 15
0 20 40 60
0 20 40
0 10 20 30 40 50
0 5 10 15 20
0 10 20 30
0 20 40

Figure 4

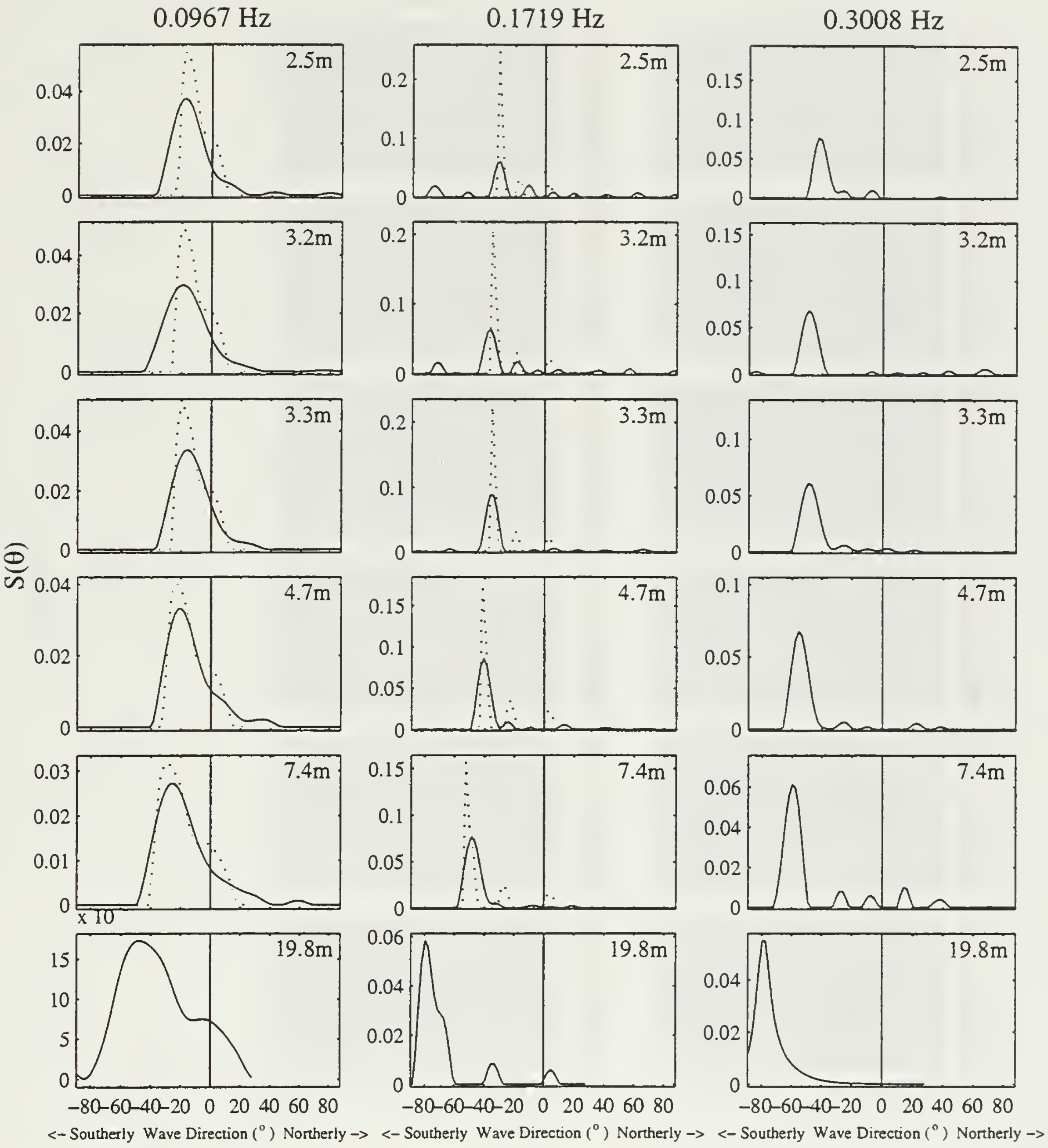
0.0967 Hz
0.1719 Hz
0.3008 Hz
2.5m
3.2m
3.3m
4.7m
7.4m
19.8m
S(θ)
x 10
0
0.01
0.02
0.03
0.04
0.05
0.06
0.1
0.15
0.2
5
10
15
-80-60-40-20 0 20 40 60 80
<-- Southerly Wave Direction (°) Northerly -->

Figure 5

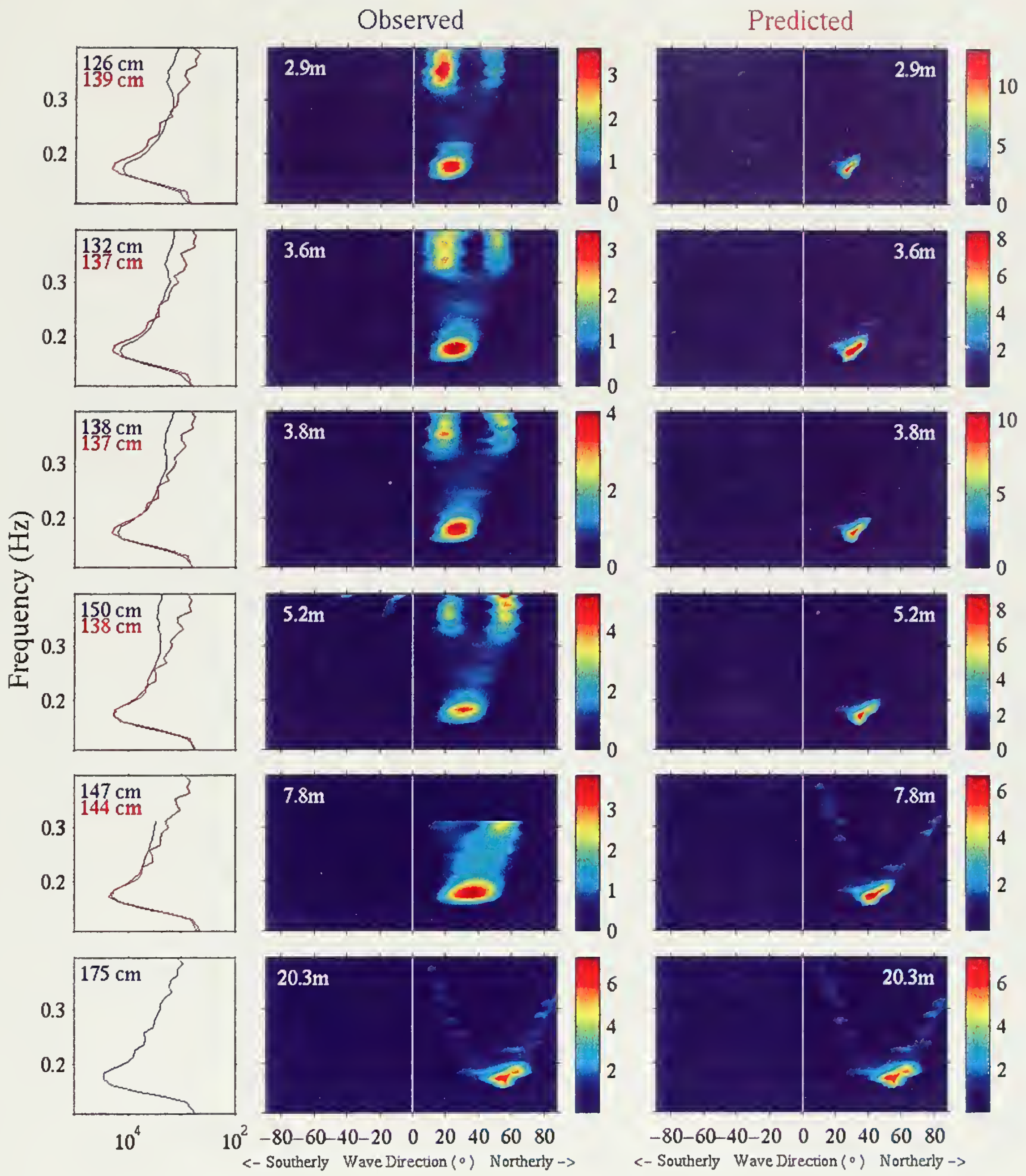
Observed
Predicted
Frequency (Hz)
0.3
0.2
126 cm
139 cm
132 cm
137 cm
138 cm
137 cm
150 cm
138 cm
147 cm
144 cm
175 cm
2.9m
3.6m
3.8m
5.2m
7.8m
20.3m
10^4
10^2
−80 −60 −40 −20 0 20 40 60 80
<- Southerly Wave Direction (°) Northerly ->
0 1 2 3 4 5 6 8 10

Figure 6

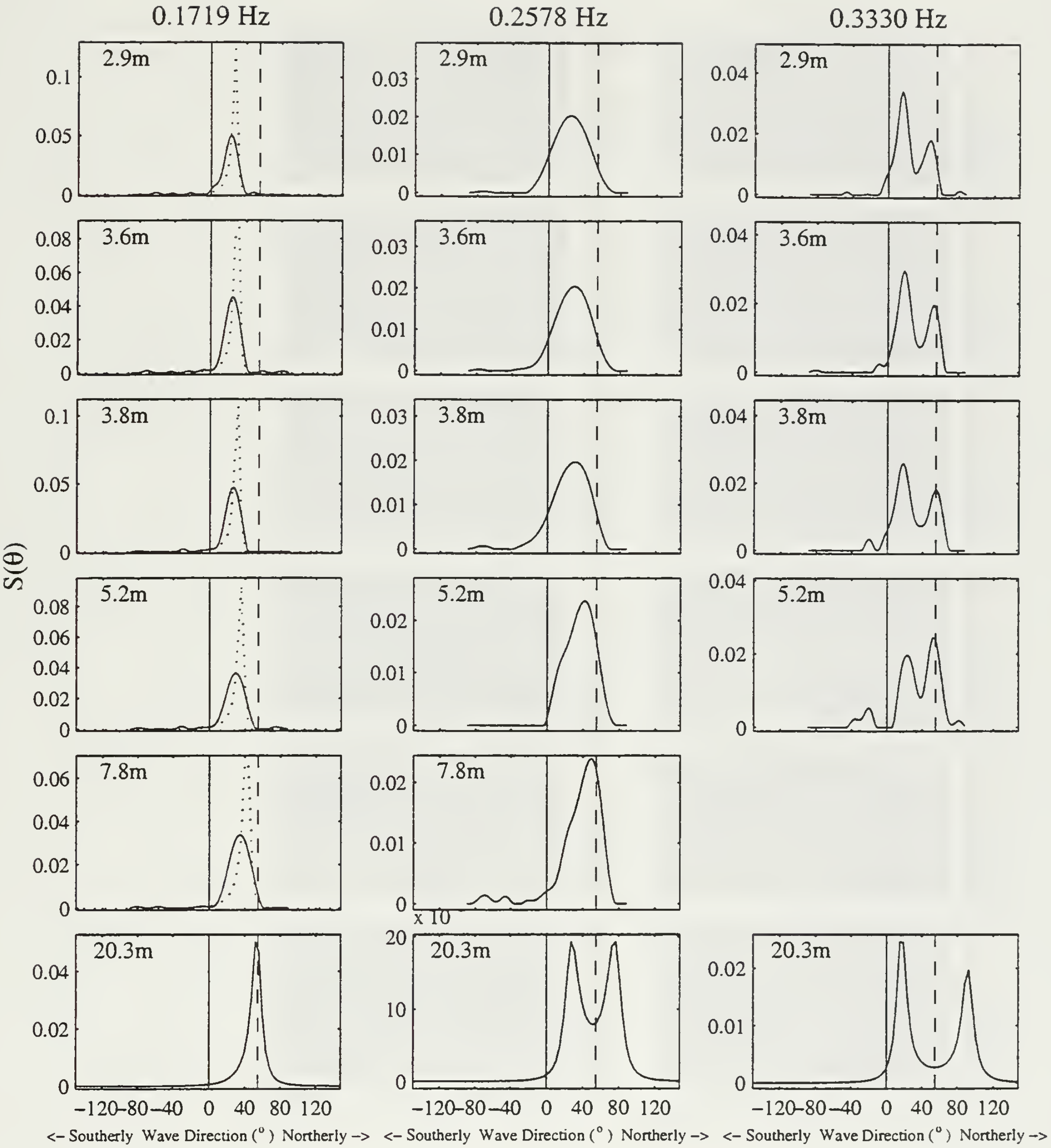
0.1719 Hz
0.2578 Hz
0.3330 Hz
2.9m
3.6m
3.8m
5.2m
7.8m
20.3m
S(θ)
0.1
0.05
0
0.08
0.06
0.04
0.02
0.03
0.01
x 10
20
10
−120−80−40 0 40 80 120
<– Southerly Wave Direction (°) Northerly –>

Figure 7

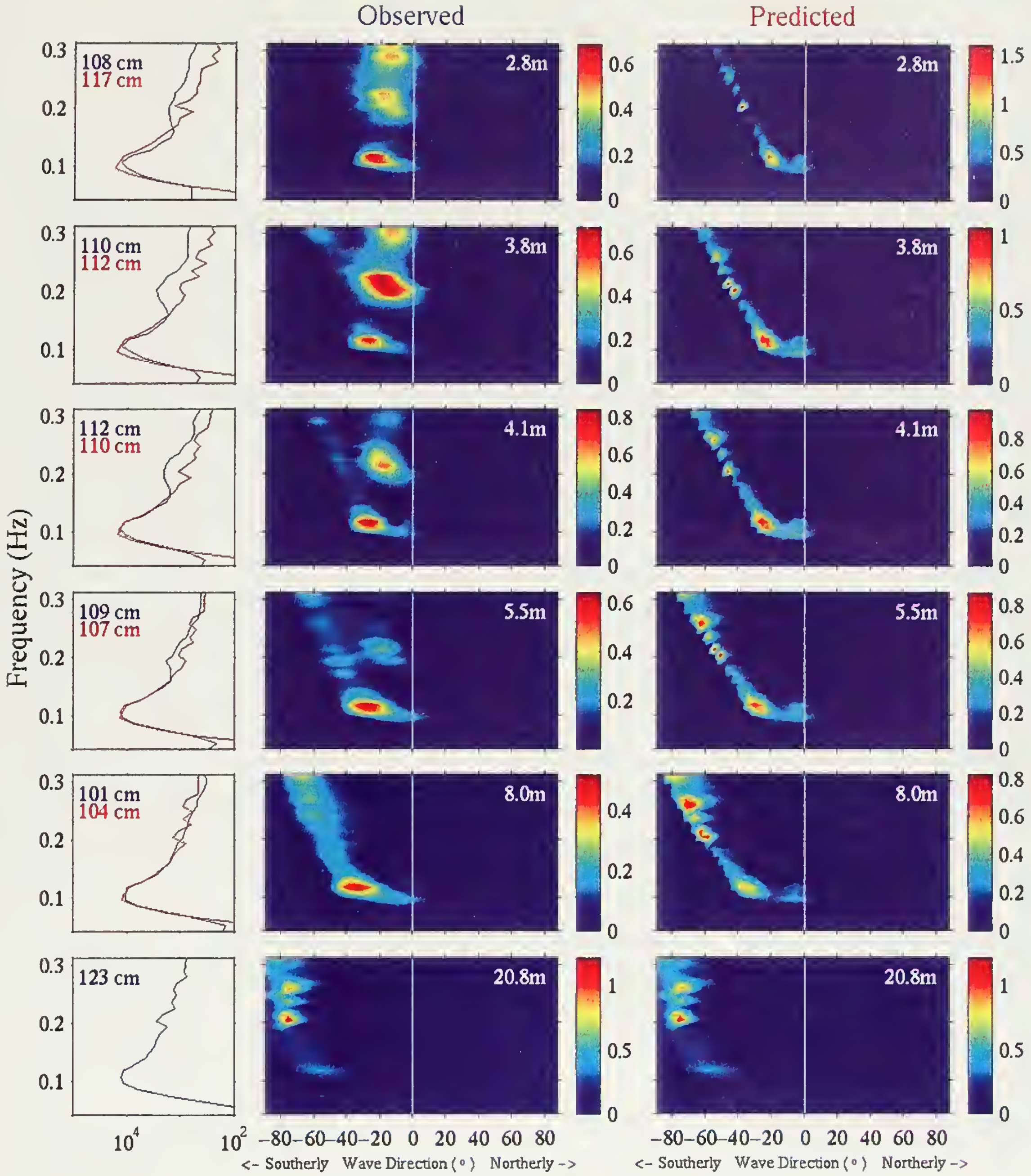

Observed
Predicted
Frequency (Hz)
0.3
0.2
0.1
108 cm
117 cm
110 cm
112 cm
112 cm
110 cm
109 cm
107 cm
101 cm
104 cm
123 cm
2.8m
3.8m
4.1m
5.5m
8.0m
20.8m
10^4
10^2
−80−60−40−20 0 20 40 60 80
<- Southerly Wave Direction (°) Northerly ->
0
0.2
0.4
0.6
0.8
0.5
1
1.5

Figure 8

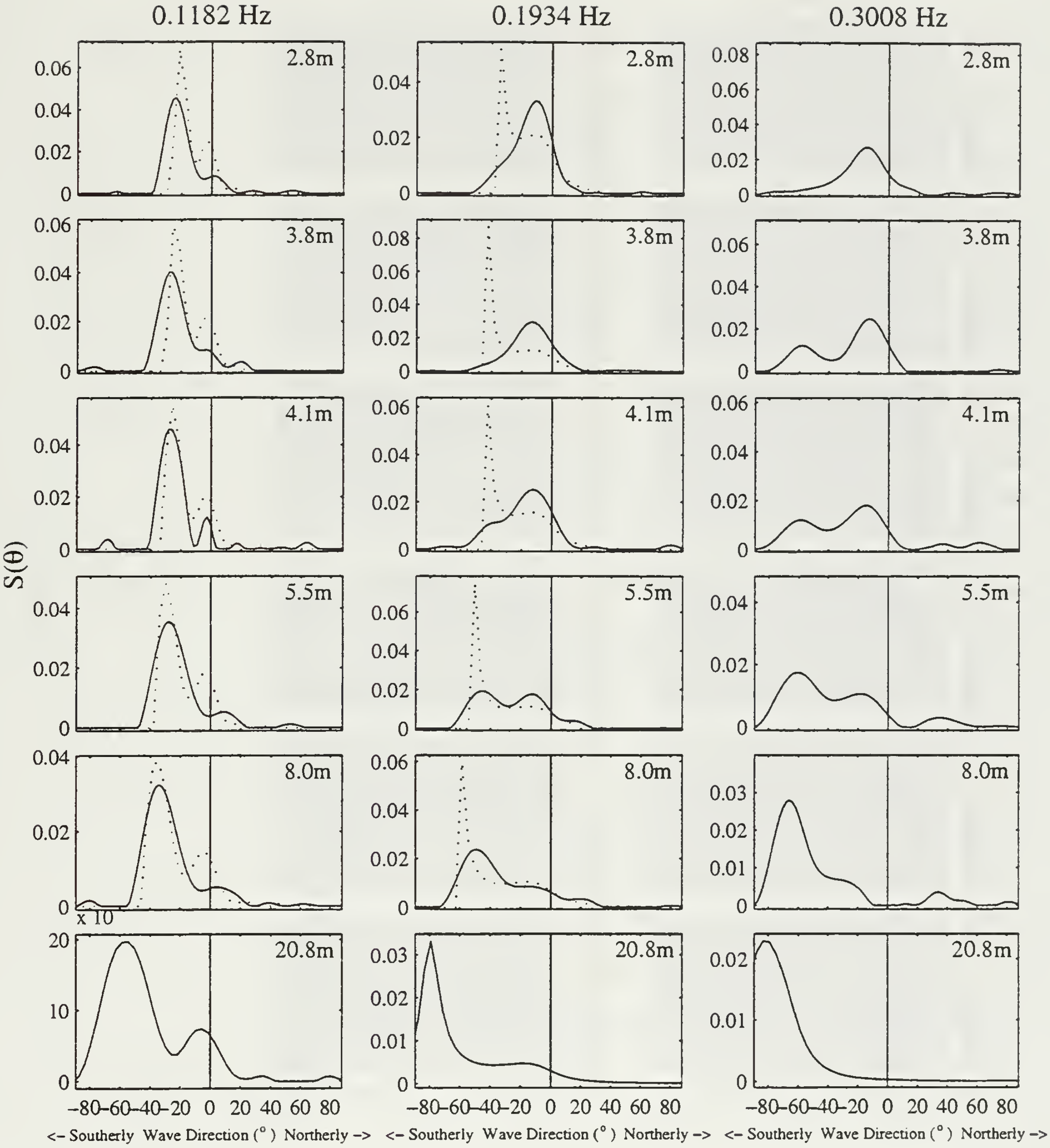
0.1182 Hz
0.1934 Hz
0.3008 Hz
2.8m
3.8m
4.1m
5.5m
8.0m
20.8m
S(θ)
x 10
0
0.01
0.02
0.03
0.04
0.06
0.08
10
20
−80−60−40−20 0 20 40 60 80
<– Southerly Wave Direction (°) Northerly –>

Figure 9

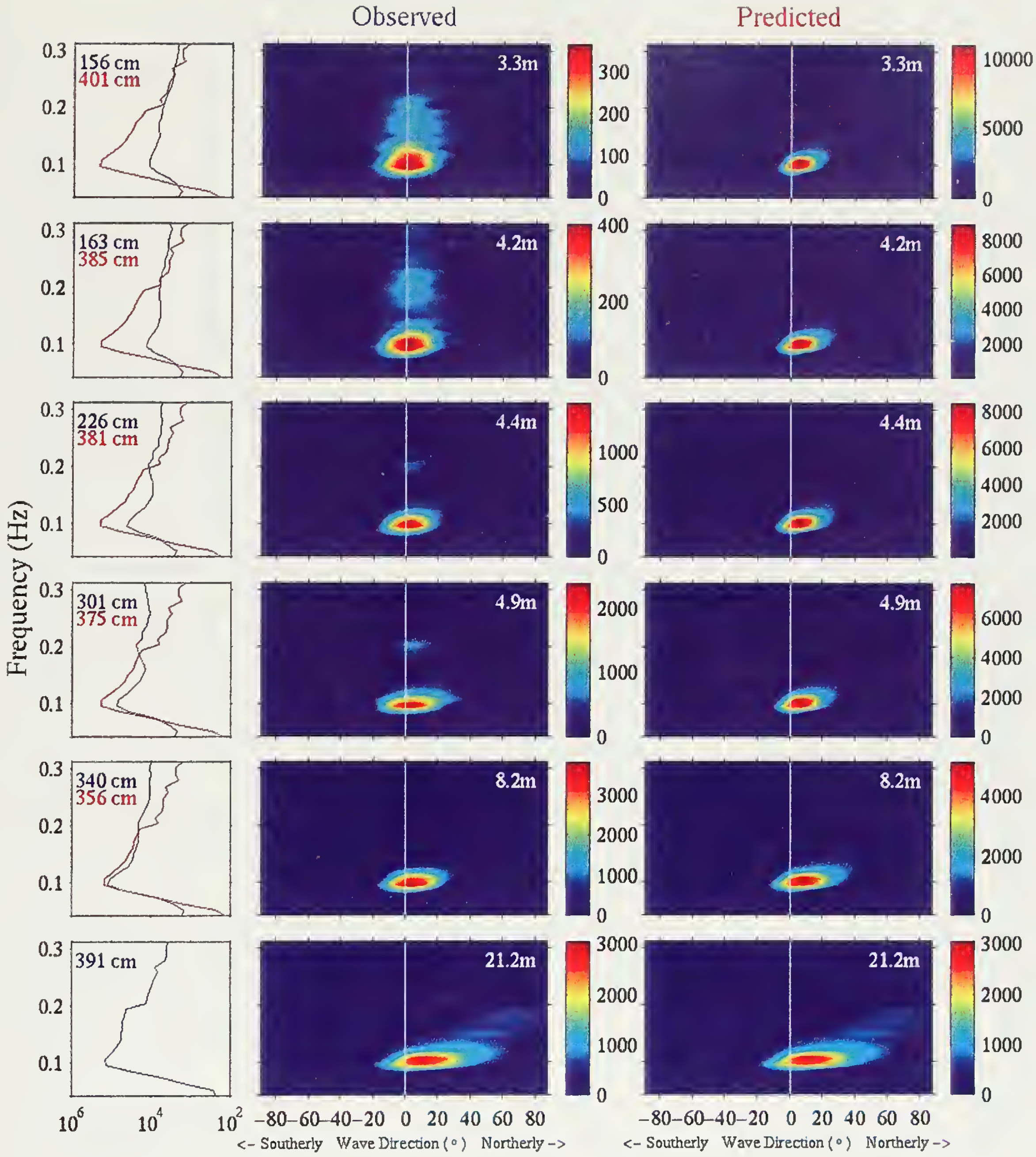
Observed
Predicted
156 cm
401 cm
3.3m
3.3m
300
200
100
0
10000
5000
0
163 cm
385 cm
4.2m
4.2m
400
200
0
8000
6000
4000
2000
226 cm
381 cm
4.4m
4.4m
1000
500
0
8000
6000
4000
2000
301 cm
375 cm
4.9m
4.9m
2000
1000
0
6000
4000
2000
0
340 cm
356 cm
8.2m
8.2m
3000
2000
1000
0
4000
2000
0
391 cm
21.2m
21.2m
3000
2000
1000
0
3000
2000
1000
0
0.3
0.2
0.1
Frequency (Hz)
10^6
10^4
10^2
−80 −60 −40 −20 0 20 40 60 80
<- Southerly Wave Direction (°) Northerly ->
−80 −60 −40 −20 0 20 40 60 80
<- Southerly Wave Direction (°) Northerly ->

Figure 10

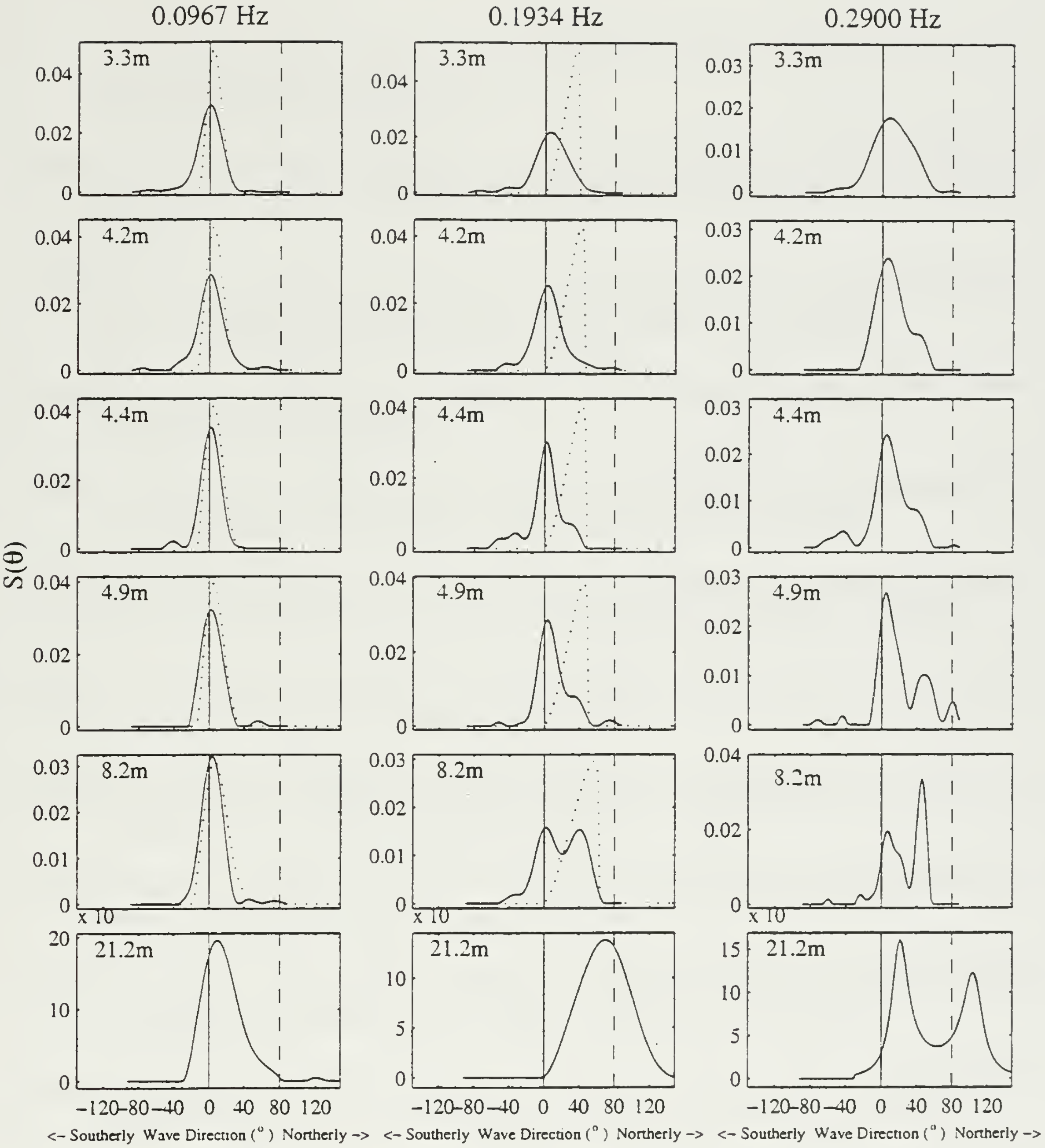
0.0967 Hz
0.1934 Hz
0.2900 Hz
3.3m
4.2m
4.4m
4.9m
8.2m
21.2m
S(θ)
0.04
0.03
0.02
0.01
0
x 10
20
15
10
5
-120 -80 -40 0 40 80 120
<- Southerly Wave Direction (°) Northerly ->

Figure 11

LIST OF REFERENCES

Ewans, K.C., 1998, "Observations of the directional spectrum of fetch-limited waves", *J.Phys. Oceanogr.*, 28, 495-512.

Freilich, M.H., Guza, R.T. and Elgar, S., 1990, "Observations of nonlinear effects in directional spectra of shoaling gravity waves", *J. Geophys. Res.*, 95, 9645-9656.

Gallagher, E., Boyd, B., Elgar, S., Guza, R.T., and Woodward, B.T., 1996, "Performance of a sonar altimeter in the nearshore", *Mar. Geol.*, 133, 241-248.

Hendrickson, E. J., 1996, "Swell propagation across a wide continental shelf", Naval Postgraduate School Thesis.

Herbers, T.H.C., and Guza, R.T., 1990, "Estimation of directional wave spectra from multicomponent observations", *J. Phys. Oceanogr.*, 20, 1703-1723.

Herbers, T.H.C., and Guza, R.T., 1991, "Wind-wave nonlinearity observed at the sea floor, part 1, forced wave energy", *J. Phys. Oceanogr.*, 21(12), 1740-1761.

Herbers, T.H.C., Elgar, S., and Guza, R.T., 1998, "Directional spreading of waves in the nearshore", in press, *J. Geophys. Res.*, 1998.

Kinsman, B., 1965, "Wind waves: Their generation and propagation on the ocean surface", Prentice Hall, Englewood Cliffs, N.J., 676 pp.

LeMéhauté, B., and Wang, J.D., 1982, "Wave spectrum changes on a sloped beach", *J. Wtrwy., Port, Coast, and Oc. Engrg.*, 108(1), 33-47.

Long, R.B., 1980, "The statistical evaluation of directional spectrum estimates derived from pitch-roll measurements", *J. Phys. Oceanogr.*, 10, 944-952.

Longuet-Higgins, M.S., 1957, "On the transformation of a continuous spectrum by refraction", *Proc. of the Cambridge Philosophical Society*, 53(1), 226-229.

Lygre, A and Krogstad, H.E., 1986, "Maximum entropy estimation of the directional distribution in ocean wave spectra", *J. Phys. Oceanogr.*, 16, 2052-2060.

Young, I.R., Verhagen, L.A. and Banner, M.L., 1995, "A note on the bimodal directional spreading of fetch-limited wind waves", *J. Geophys. Res.*, 100, 773-778.

INITIAL DISTRIBUTION LIST

1. Defense Technical Information Center 2
   8725 John J. Kingman Rd., Ste 0944
   Ft. Belvoir, VA 22060-6218

2. Dudley Knox Library 2
   Naval Postgraduate School
   411 Dyer Rd.
   Monterey, CA 93943-5101

3. Professor T.H.C. Herbers, Code OC/He 8
   Department of Oceanography
   Naval Postgraduate School
   Monterey, CA 93943 - 5121

4. Professor E.B. Thornton, Code OC/Tm 1
   Department of Oceanography
   Naval Postgraduate School
   Monterey, CA 93943 - 5121

5. Matthew I. Borbash 1
   1017 Neal Drive
   Rockville, MD 20850

12 483NPG 3104
TH
10/99 22527-200 NULE
ICI INFORMATION CONSERVATION INC

DUDLEY KNOX LIBRARY
3 2768 00368290 7